ATLAS NOTE

October 27, 2017

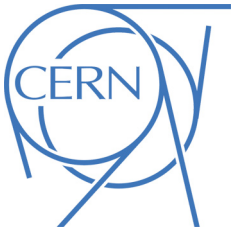

Simple Simulation of the Micromegas Trigger at High Rates, and a Proposal for Improving the ϕ Measurement

J. Farah[a,b], N. Felt[a], M. Franklin[a], P. Giromini[a], J. Philion[a], A. Tuna[a], A. Wang[a]

[a] *Harvard University, Cambridge, Massachusetts 02138, USA*
[b] *University of Massachusetts Boston, Boston, Massachusetts 02125, USA*

Abstract

We simulated the MM Trigger Processor at high rates. We can improve the non-precision measurement dramatically.

1 Introduction

Introduction.

2 Micromegas detector and electronics

Micromegas detector and electronics.

Test stand measurements.

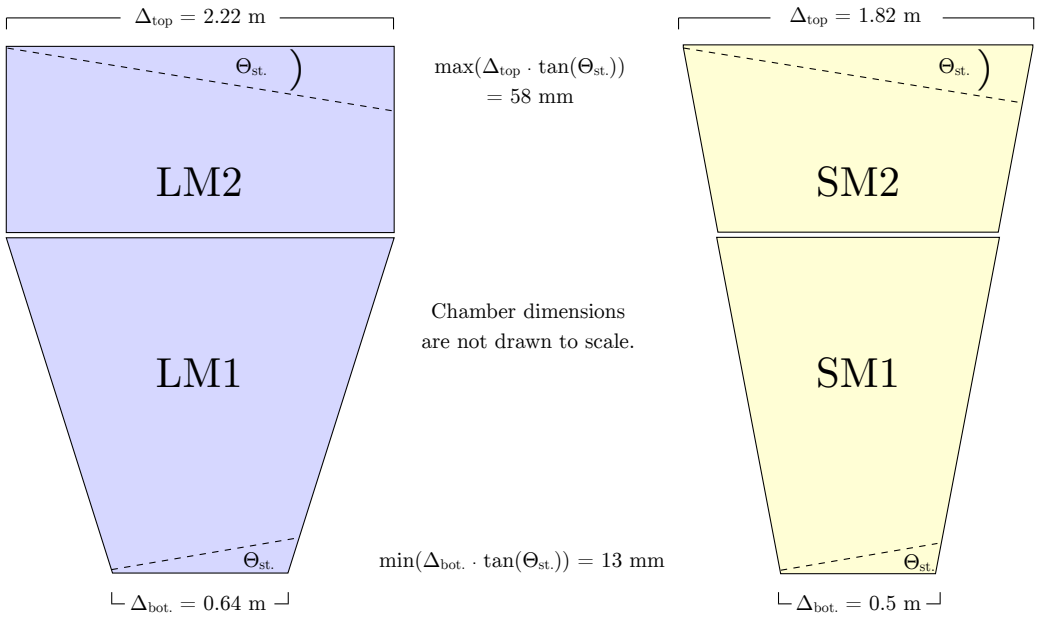

Figure 1: Drawings of Micromegas wedges with dimensions as specified by the NSW TDR. The stereo strips require larger roads than the horizontal strips because they overlap a band of x strips of width from 13 to 58 mm.

3 High luminosity LHC

HL-LHC conditions.

4 Simulation

Standalone simulation.

Effects considered. Faithfulness of the software implementation.

5 Nominal algorithm

Nominal algorithm and performance.

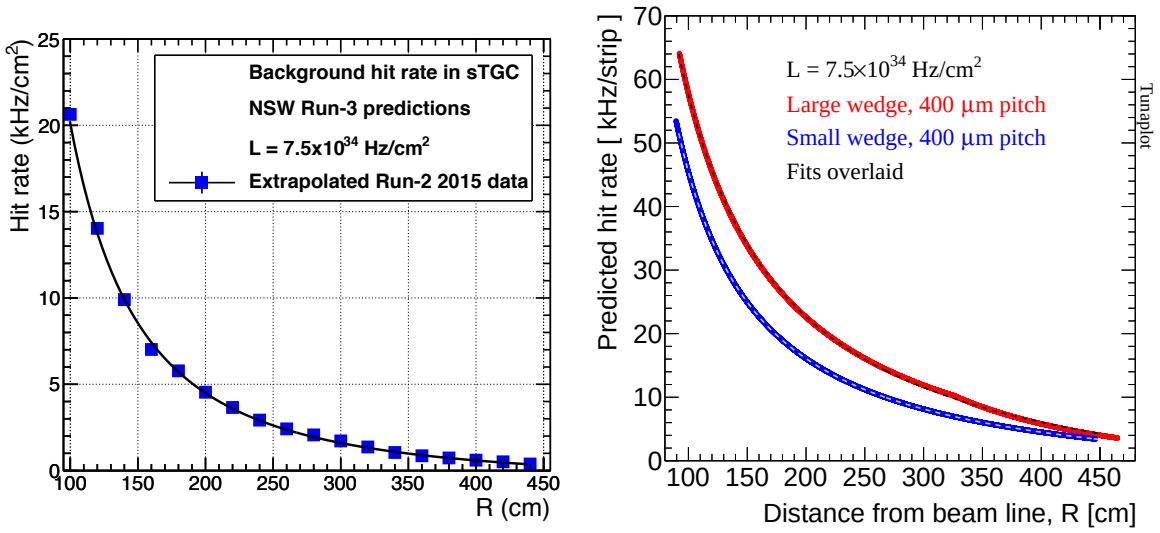

Figure 2: Predicted rate vs. distance from the beamline at $\mathcal{L} = 7.5 \times 10^{34}$ Hz/cm^2, per unit area (left) and per strip (right). The rate per area is culled from the Phase 2 Muon TDR [10]. The rate per strip is derived from the rate per area and the expected area of the Micromegas chambers.

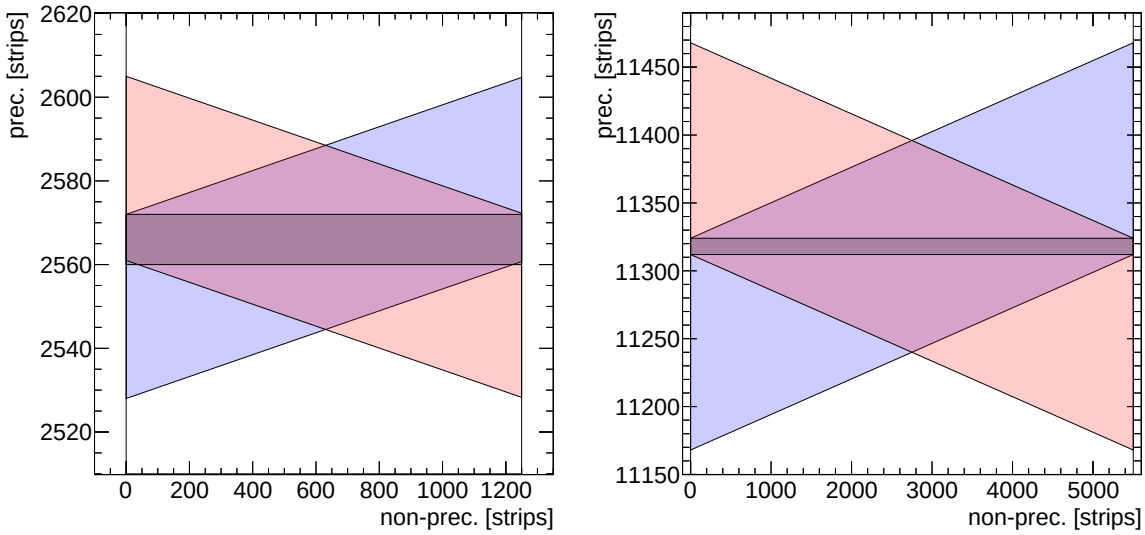

Figure 3: Sketch of the road coverage of the nominal MMTP algorithm, for a small chamber closest to the beamline (left) and large chamber farthest from the beamline (right). The *X* road is horizontal, the *U* road is pink and slanted, and the *V* road is blue and slanted.

6 Small stereo roads

Proposal and performance of small stereo roads.

7 Hardware resources

FPGA resources.

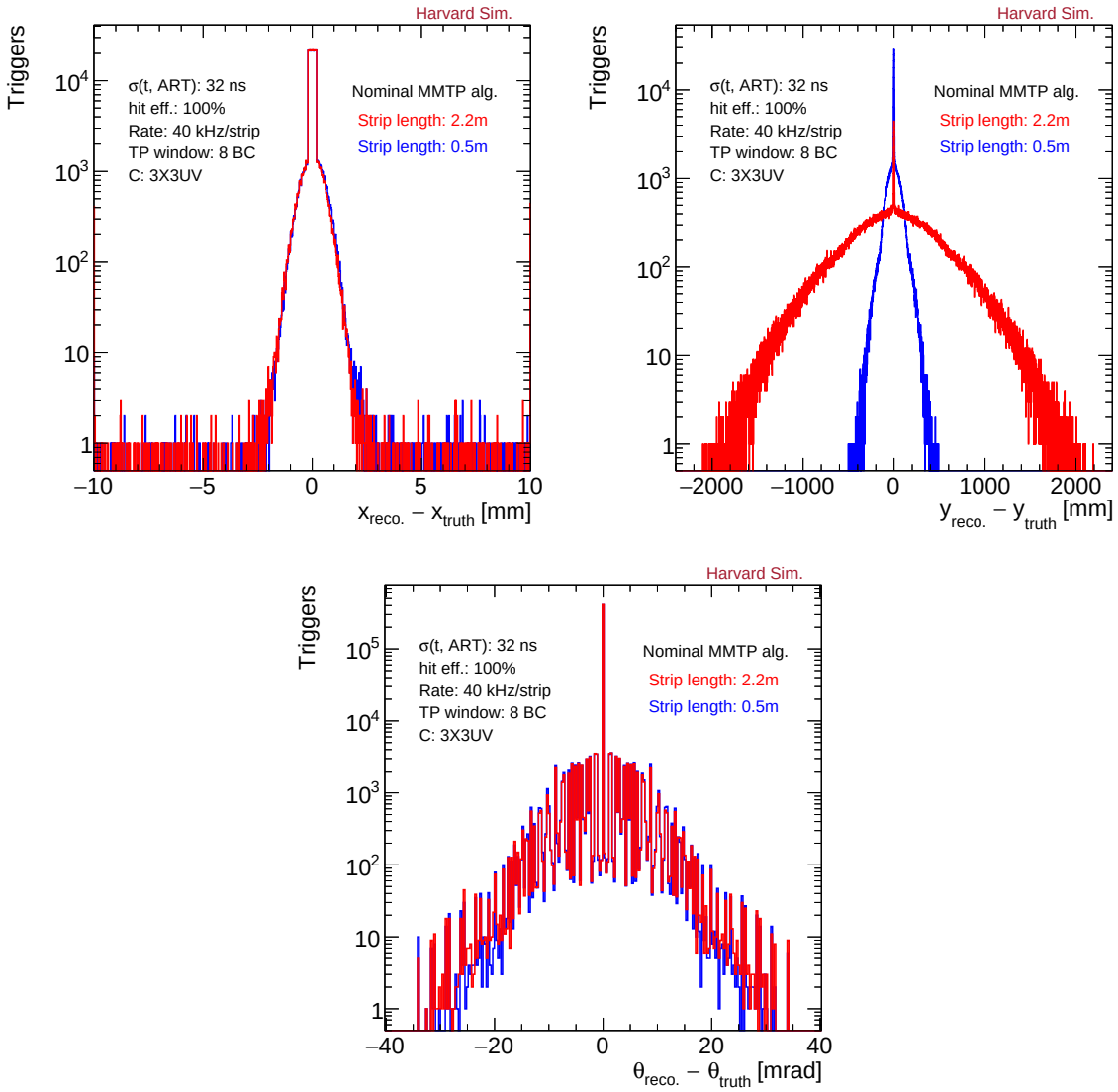

Figure 4: Distribution of $x_{\text{reco.}} - x_{\text{truth}}$ (top, left), $y_{\text{reco.}} - y_{\text{truth}}$ (top, right) and $\theta_{\text{reco.}} - \theta_{\text{truth}}$ (bottom) for the nominal MMTP algorithm with uncorrelated background at a rate of 40 kHz per strip.

8 Conclusion

Conclusion.

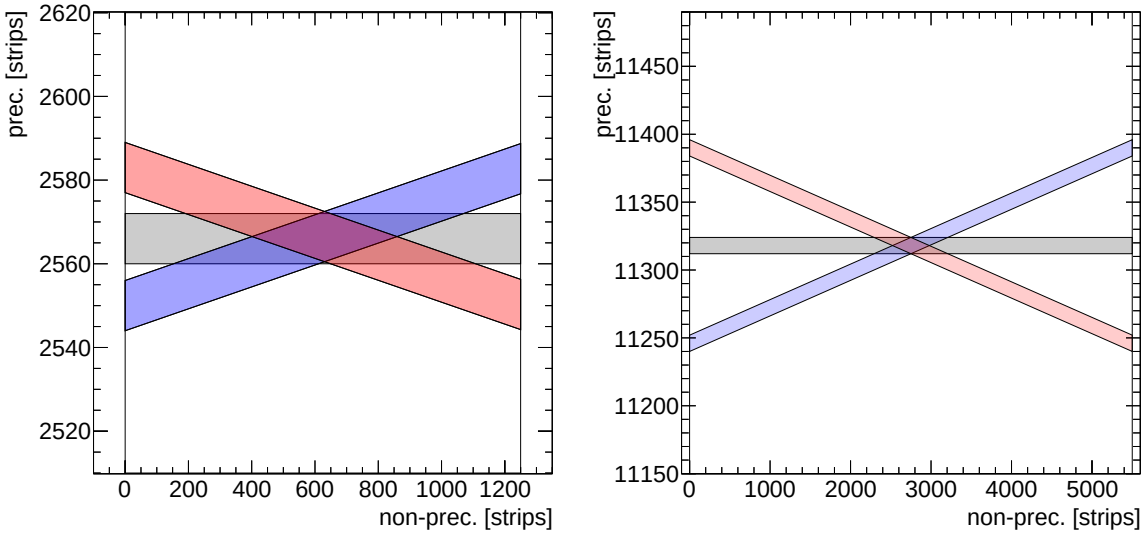

Figure 5: Sketch of the road coverage of the proposed MMTP algorithm, for a small chamber closest to the beamline (left) and large chamber farthest from the beamline (right). The *X* road is horizontal, the *U* road is pink and slanted, and the *V* road is blue and slanted. For ease of digestion, only one pair of *U* and *V* roads are shown, and they do not cover the entire *X* road.

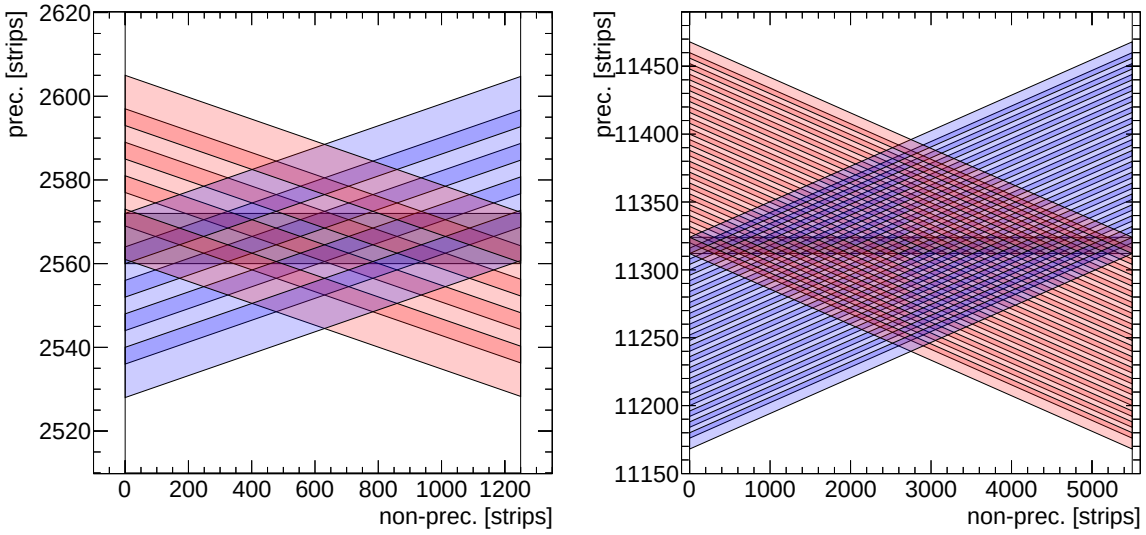

Figure 6: Sketch of the road coverage of the proposed MMTP algorithm, for a small chamber closest to the beamline (left) and large chamber farthest from the beamline (right). The *X* road is horizontal, the *U* roads are pink and slanted, and the *V* roads are blue and slanted. The small chamber requires five pairs of *U* and *V* roads to cover one *X* road, and the large chamber requires 19.

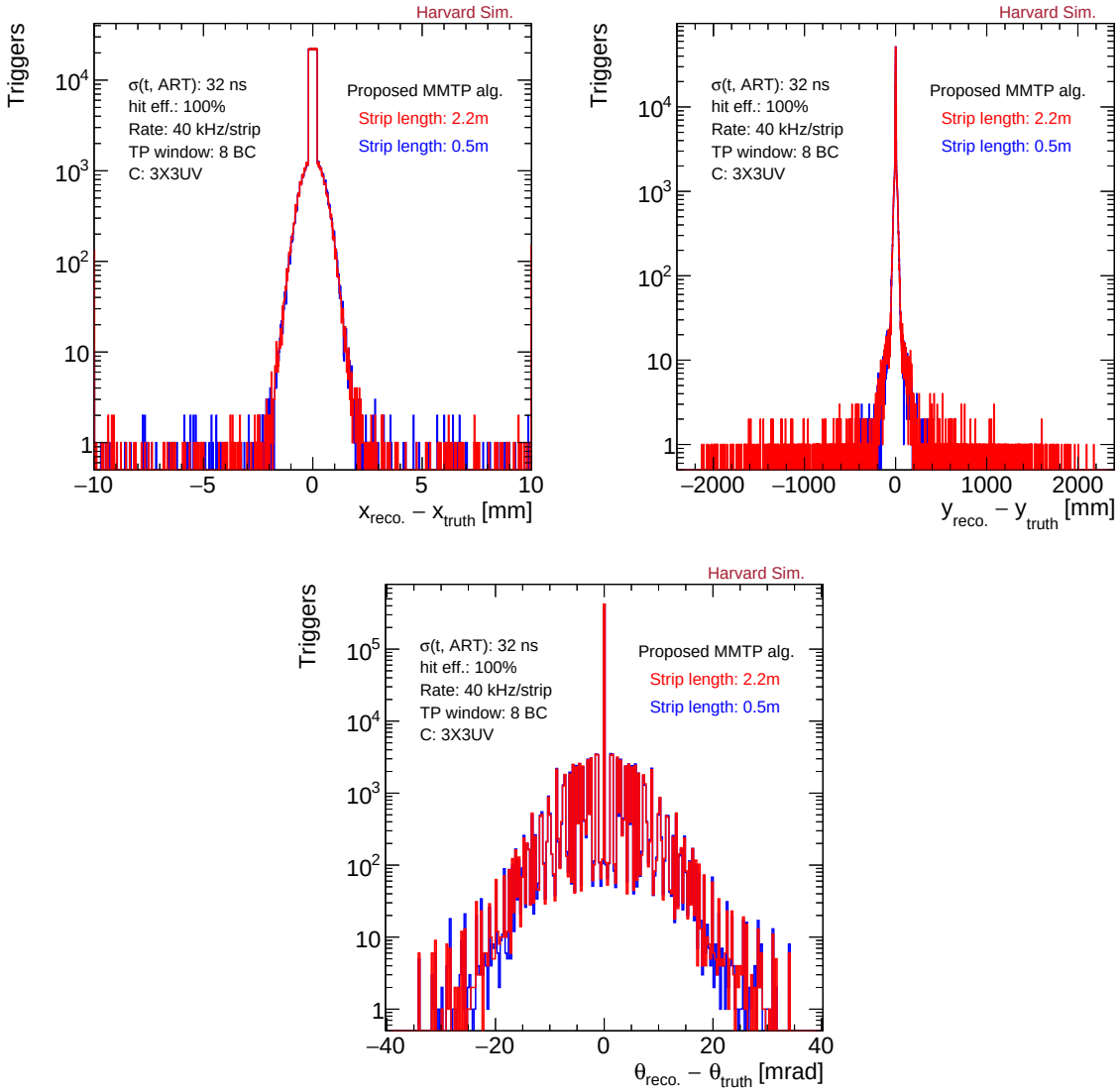

Figure 7: Distribution of $x_{\text{reco.}} - x_{\text{truth}}$ (top, left), $y_{\text{reco.}} - y_{\text{truth}}$ (top, right) and $\theta_{\text{reco.}} - \theta_{\text{truth}}$ (bottom) for the nominal MMTP algorithm with uncorrelated background at a rate of 40 kHz per strip.

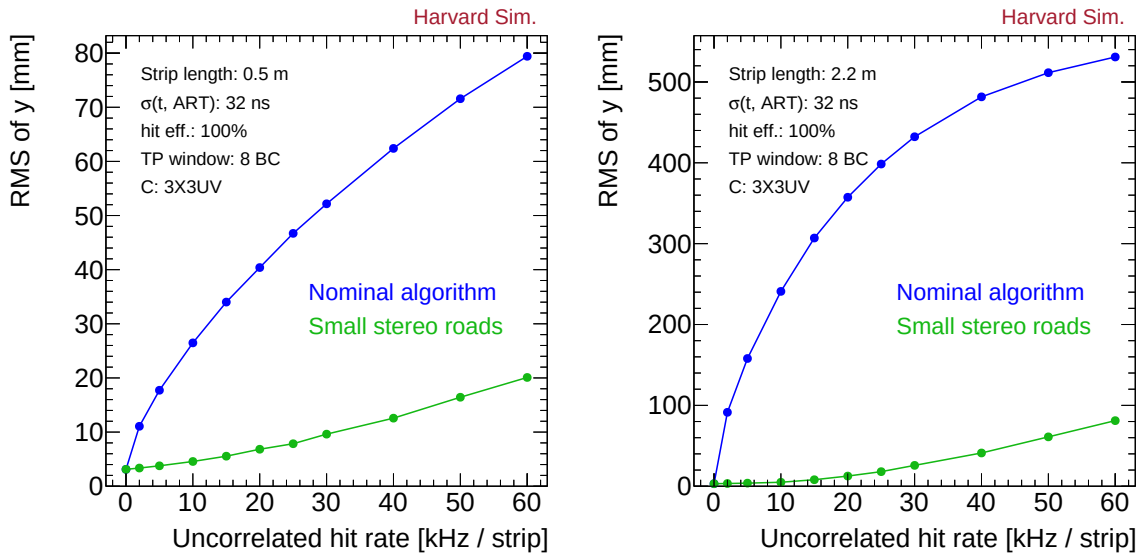

Figure 8: RMS of $y_{\text{reco.}} - y_{\text{truth}}$ for a small chamber of width 0.5m (left) and large chamber of width 2.2m (right) as a function of uncorrelated background rate. The RMS is calculated in the 3σ (99.7%) range of the distribution.

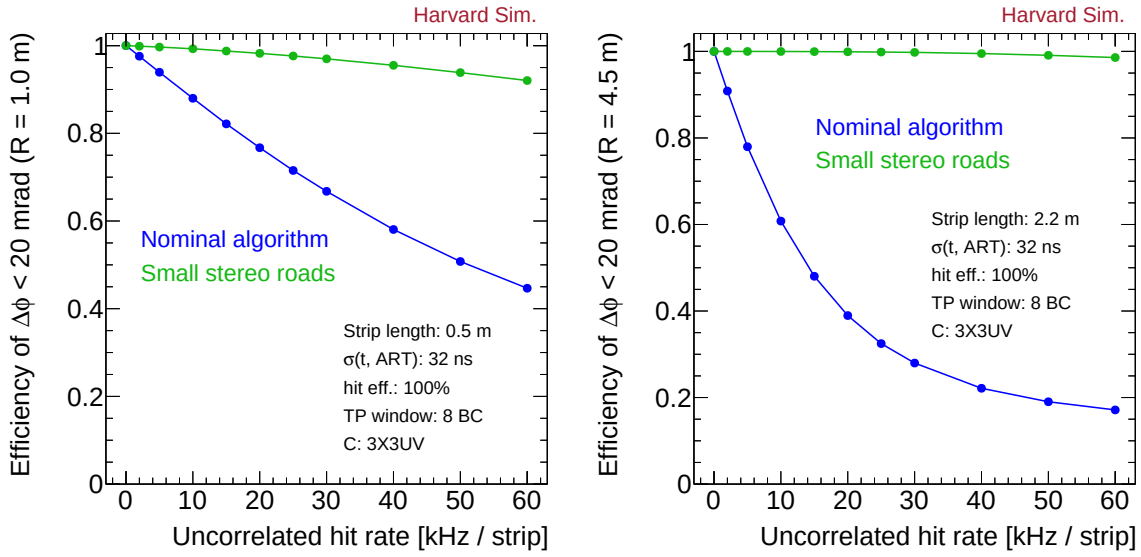

Figure 9: Efficiency of $\phi_{\text{reco.}} - \phi_{\text{truth}} < 20$ mrad for a small chamber (left) and large chamber (right). $\phi_{\text{reco.}} - \phi_{\text{truth}}$ is calculated as $\frac{y_{\text{reco.}} - y_{\text{truth}}}{R}$, where R is the distance from the beamline. R is taken to be 1m for the small chamber and 4.5m for the large chamber.

References

[1] ATLAS New Small Wheel Technical Design Report. ATLAS-TDR-020. ATL-COM-MUON-2017-036.

[2] P. Giromini *et al,* Performance of a Micromegs octuplet in the time of noise. ATL-COM-MUON-2017-036.

[3] P. Giromini *et al,* Performance of a Micromegs octuplet after removing the major cause of noise. ATL-COM-MUON-2017-040.

[4] `https://twiki.cern.ch/twiki/bin/viewauth/Atlas/NewSmallWheel`.

[5] `https://twiki.cern.ch/twiki/pub/Atlas/February_2015_design_reviews/ADDC_document_for_2015_Feb_NSW_review_v1.0.pdf`.

[6] B. Clark *et al,* An Algorithm for Micromegas Segment Reconstruction in the Level-1 Trigger of the New Small Wheel. ATL-COM-UPGRADE-2014-012.

[7] S. Chan et. al. Micromegas Trigger Processor Algorithm Performance in Nominal, Misaligned, and Misalignment Corrected Conditions. ATL-COM-UPGRADE-2015-033.

[8] K. DiPetrillo it et al, ATL-COM-MUON-2014-069.

[9] Simulation of the ATLAS New Small Wheel (NSW) System ATL-MUON-SLIDE-2017-248.

[10] ATLAS Muon Spectrometer Phase-II Upgrade Technical Design Report. ATL-COM-MUON-2017-033.